Fouling propensity of forward osmosis: investigation of the slower flux decline phenomenon

Winson C. L. Lay, Tzyy Haur Chong, Chuyang Y. Tang, Anthony G. Fane, Jinsong Zhang and Yu Liu

ABSTRACT

Forward Osmosis (FO) is a membrane process that uses the natural osmotic pressure of a concentrated draw solution to extract pure water from a feed stream. The attraction of the FO process is that it uses dense membranes, while operating at ambient pressure. This means that the FO process could potentially produce high quality water with lower energy consumption, as compared to the other desalination or reclamation processes. As FO does not entail the use of hydraulic pressure, FO has been hypothesized to have lower fouling propensity than pressure driven membrane processes. Membrane fouling has significant impact on the operational sustainability and economics of the process. This study examines the possible contributing factors to the slower flux decline observed in FO experiments based on a combined experimental and modelling approach. It was found that these factors could include low water fluxes, use of hydrophilic and smooth membranes, and the effect of internal concentration polarisation that is inherent of FO. It was also found that the transmission of draw solutes from the draw solution into the feed can have significant effect on FO performance.

Key words | desalination, forward osmosis, fouling, internal concentration polarisation, water reclamation

Winson C. L. Lay
Tzyy Haur Chong
Chuyang Y. Tang
Anthony G. Fane (corresponding author)
Jinsong Zhang
Yu Liu
Singapore Membrane Technology Centre,
Nanyang Technological University,
Singapore 639798,
Singapore

Winson C. L. Lay
Chuyang Y. Tang
Anthony G. Fane (corresponding author)
Yu Liu
Division of Environmental and Water Resources Engineering,
School of Civil and Environmental Engineering,
Nanyang Technological University,
Singapore 639798,
Singapore
E-mail: *agfane@ntu.edu.sg*

INTRODUCTION

Forward Osmosis (FO) is a membrane process that uses the natural osmotic pressure of a concentrated draw solution to extract pure water from a feed stream. As early as the 1960s, FO has been viewed with interest as a promising technology for both water treatment and energy generation, the latter which is known as pressure-retarded osmosis (PRO). However, significant developments in FO/PRO have mostly taken place in the last decade, alongside the general advancement of membrane technology. Recent developments and new concepts for FO in the applications of seawater desalination (McCutcheon *et al.* 2005) and used water treatment (Wessels & Cornelissen 2005) have rekindled interest in the process. The attraction of the FO process is that it uses dense membranes, comparable to those used in the Reverse Osmosis (RO) process, while operating at ambient pressure. This has the positive implication that the FO process could potentially produce high quality water with lower energy consumption, as compared to the other desalination or reclamation processes.

Membrane fouling has significant impact on the operational sustainability and economics of the process. Lower membrane fouling implies longer operation and more water production, less cleaning and longer membrane life. In practical terms, this will mean reduction in both operation and capital costs, and could further enhance the attractiveness of the FO process for large-scale applications. As FO does not entail the use of hydraulic pressure, there is literature reporting that FO may have lower fouling propensity than pressure driven membrane

doi: 10.2166/wst.2010.835

processes (Holloway *et al.* 2007; Oo *et al.* 2008; Achilli *et al.* 2009). Part of this hypothesis is construed on the observation of slower flux decline in FO experiments. The explanation offered was that fouling cake-layer compaction would be reduced in the absence of hydraulic pressure. The scientific implication of this view is that there is a difference in the relative impact on foulant compaction by flux and pressure. Such a view, however, could be contradictory to the well established critical flux concept (Field *et al.* 1995), which gives pressure as the driving force, but it is the drag force of the moving fluid (flux) that acts as the agent for fouling. What this means is that regardless of the type of driving force, the effect of membrane fouling should be comparable under similar flux and operational conditions.

The objective of this study was to investigate and understand the fouling propensity of FO by examining possible contributing factors to the slower flux decline observed in FO experiments. The study comprised experimental and modelling work, and performed comparative analysis between FO and RO under similar fouling conditions.

MATERIALS AND METHODS

Experimental set-up and procedure

A schematic diagram of the dual-track membrane experimental system (supplied by Newton & Stokes, Singapore) used in this study is shown in Figure 1. The system comprised a high-pressure (RO) loop and a low-pressure (FO) loop. The configurations for both loops were essentially identical,

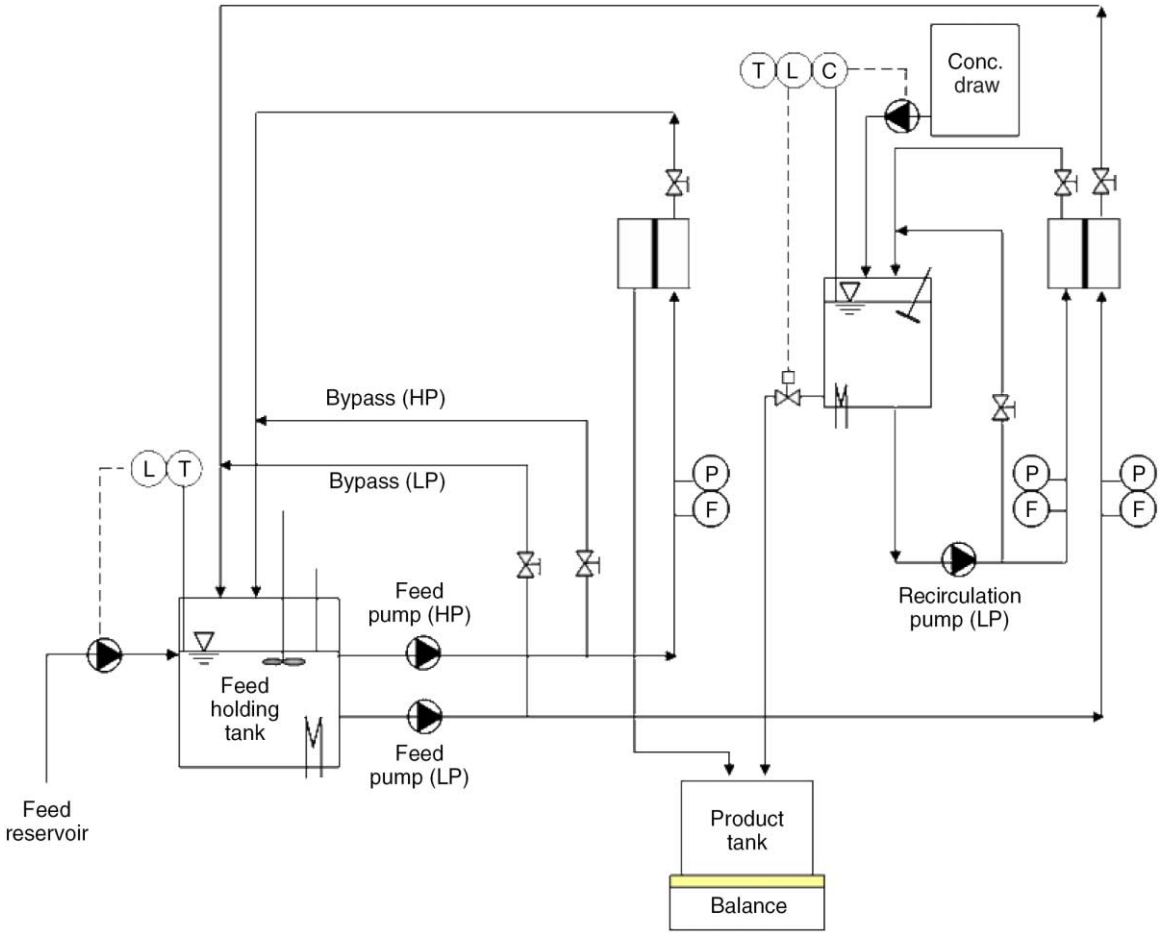

Figure 1 | Schematic diagram of the dual-track membrane experimental system.

except for the components related to the provision of the driving force. The membrane cells in both loops were custom-made of engineering plastic that could withstand high salt concentrations, and held together by parallel metal slabs. The effective membrane area for both cells was identical and given by the channel dimensions of 24.8 cm by 3.1 cm. Both cells could be run with cross flow on both sides of the membrane. For the RO cell, the inlet valve on the permeate side was closed to give the standard RO configuration. For the FO cell, cross flow were run on both the feed and the draw side co-currently to minimise mechanical strain on the membrane. The driving force for the RO loop was supplied by a high-pressure pump (Speck Triplex NP10/10-140S) that generated feed-side pressures up to 20 bars. The driving force for the FO loop was supplied by re-circulating sodium chloride (NaCl) draw solution, which was maintained at constant concentration by means of a conductivity control linked to a concentrated NaCl (5 molal) solution reservoir. The NaCl solution was used here as the draw solution, as it is typically the appropriate choice that satisfies the required criteria: high solubility and osmotic pressure efficiency, chemically compatible, easy to regenerate and no risk of scaling (Cath *et al.* 2006).

Fluid conveyance in the FO loop was provided by centrifugal pumps (Calpeda NMX 32/125AE), and the transmembrane hydraulic pressure difference was less than 0.1 bar, which was insignificant as compared to the osmotic pressure difference. Flows in the system were adjusted by valves located on the main and the bypass lines, which gave feed-side cross flow velocities in the order of 0.1 ms^{-1}. For the FO loop, the draw-side was set after adjusting the feed-side cross flow velocity and the pressures on both sides of the membrane, and was in the order of 0.5 ms^{-1} for the experiments. The feed water temperature for the experiments was maintained between 24°C and 26°C by the system chillers. For RO experiments, product water was collected and measured directly by a weighing balance (AND GX-30K). For FO experiments, product collection was performed by a level control in the product holding tank connected to the weighing balance through a solenoid valve. The product water flux in $Lm^{-2}h^{-1}$ (LMH) was then derived by normalising the measured product rate over the membrane area, correcting with the amount of draw solution dosed into the system and accounting for the density of the draw solution. Osmotic pressure was measured by a cryoscopic osmometer (Gonotec OSMONAT 030) up to 3 Osmol/kg (~1.5 molal NaCl) or derived from the literature for higher osmotic pressure values (Robinson & Stokes 2002). Outputs of the parameters: pressures, flow rates, temperatures, conductivity and product collection were obtained via a data acquisition system (IDEC PLC with LabVIEW).

The same type of membrane (cartridge type) from Hydration Technology Innovations (Albany, OR) was used in all experiments. The membrane was made of cellulose triacetate embedded about a polyester screen mesh, and was found to be the currently best available membrane for FO application (Cath *et al.* 2006). The same membrane orientation was consistently adopted in this study with the active layer facing against the feed solution. Prior to use, the membrane was cut to size and stored in Milli-Q water at 4°C overnight. A fresh piece of membrane was used in each fouling experiment.

Model foulant solution used in this study was 200 ppm of 10–20 nm silicon dioxide nanoparticles (Sigma-Aldrich). The experimental protocol was consistently applied as follows: prior to the addition of foulant, a common precompaction and equilibration step was applied to the membrane by subjecting it in the RO cell to feed pressure of 20 bar and background electrolyte concentration of 1 gL^{-1} NaCl for 2 h. For the FO experiments, the membrane was transferred to the FO cell right after the precompaction and equilibration step, and this was followed by an additional equilibration step for conditions on both the feed and the draw side to stabilise. Analysis of the experimental data was performed on the first 15 h after the addition of foulant. To reduce data noise that was associated with the data acquisition system, three-point averaging method was applied.

Process modelling

Table 1 gives an overview of the equations and parameters used in this study. Both Equations (1) and (2) are implicit functions that describe the water flux (J_w) in RO and FO respectively, and could be solved by numerical or graphical method. The basis of the modelling was the resistance-in-series model incorporated with the

Table 1 | Modelling equations and parameters

Water flux equations

Intrinsic flux given by the driving force / Flux loss due to CEOP

$$\text{RO: } J_w = \frac{A \cdot (\Delta p - \exp(\frac{J_w \cdot \delta^*}{D}) \cdot \pi_{F,B})}{(1 + \frac{R_f}{R_m})}$$

Water transport / Normalised fouling resistance

Intrinsic flux given by the driving force / ICP / Flux loss due to CEOP

$$\text{FO: } J_w = \frac{(A \cdot \pi_{D,B} + B)(\exp(-\frac{J_w \cdot S}{D})) - (A \cdot \pi_{F,B} + B)(\exp(\frac{J_w \cdot \delta^*}{D}))}{(1 + \frac{R_f}{R_m})}$$

Water transport / Normalised fouling resistance

A	[$ms^{-1}bar^{-1}$]	water permeability constant
B	[ms^{-1}]	salt permeability constant
Δp	[bar]	transmembrane (hydraulic) pressure
$\pi_{F,B}$	[bar]	osmotic pressure of the feed solution
$\pi_{D,B}$	[bar]	osmotic pressure of the draw solution
D	[$m^2 s^{-1}$]	diffusion coefficient of the solutes
δ^*	[m]	enhanced fouling cake thickness ($\delta^* = \delta_c \cdot \tau_c / \epsilon_c$)
S	[m]	membrane structural parameter ($S = t_m \cdot \tau_m / \epsilon_m$)
R_m	[m^{-1}]	membrane resistance
R_f	[m^{-1}]	fouling resistance ($R_f = \rho_p \cdot (1 - \epsilon_c) \cdot \delta_c \cdot \alpha_c$)

Salt concentration effect

$$C_{F,B} = \frac{\frac{\varphi \cdot J_s}{J_w} + C_{F,0}}{(1 - \varphi)}$$

$c_{F,B}$	[gL^{-1}]	steady state feed concentration
$c_{F,0}$	[gL^{-1}]	influent feed concentration
ϕ	[−]	system recovery (= product flow/feed flow)
J_S	[$gm^{-2}h^{-1}$]	salt flux
J_W	[$Lm^{-2}h^{-1}$]	Water flux

cake-enhanced osmotic pressure (CEOP) effect. The CEOP effect accounts for the hindered diffusion of the retained solutes in the fouling cake layer, which exponentially magnifies the feed-side osmotic pressure on the membrane wall, and thereby reduces driving force. The practical implication of CEOP is that it can greatly aggravate the impairment of membrane performance as fouling occurs. The significance of CEOP to salt retentive membrane systems

has been established in a number of studies (Hoek & Elimelech 2003; Chong *et al.* 2008*a*,*b*; Zhang *et al.* 2008).

For FO modelling, it was necessary to consider internal concentration polarisation (ICP). The ICP is an inherent phenomenon of FO that occurs within the porous support layer of the membrane and acts to reduce driving force (Lee *et al.* 1981; Loeb *et al.* 1997; McCutcheon & Elimelech 2007; Gerstandt *et al.* 2008). The ICP is given by the exponential term $\exp(-J_w \cdot S/D)$ Equation (2) At this juncture, we note the difference in the nature of the driving force between RO and FO. For RO, the intrinsic flux given by the driving force is $A \cdot \Delta p$ (Equation 1), and is constant for a given driving force (Δp). For FO, however, the intrinsic flux depends on the product of $(A \cdot \pi_{D,B} + B)$ and ICP (Equation 2). So, even when the overall driving force for a FO process ($\pi_{D,B}$) is constant, the effective driving force changes according to the ICP. This explains the logarithmic relationship between the water flux and the overall driving force for the FO process, and that any change in flux has a direct and inverse impact on the effective driving force across the membrane.

Salt concentration occurs in all salt retentive membrane systems, as pure water permeates through the membrane, leaving behind the concentrate and elevating the osmotic pressure of the feed solution. For FO, this effect is intensified due to the salt flux that is transmitted from the draw solution into the feed solution. From a system mass balance for the salt component, Equation (3) could be derived. The salt flux (J_s) could be derived from the solutions diffusion theory. Note that Equation (3) is also valid for RO, when $J_s = 0$. The reference salt used throughout this study for the total dissolved solids (TDS) contained in the feed solution and for the draw solution is NaCl.

RESULTS AND DISCUSSION

Result from FO–RO experiments

Figure 2 gives the normalised flux decline over time of the experiments. The baseline for the normalisation was set to an assumed steady-state flux (J @ $t = 2$ h), so as to take into the account the initial flux drop in FO as explained

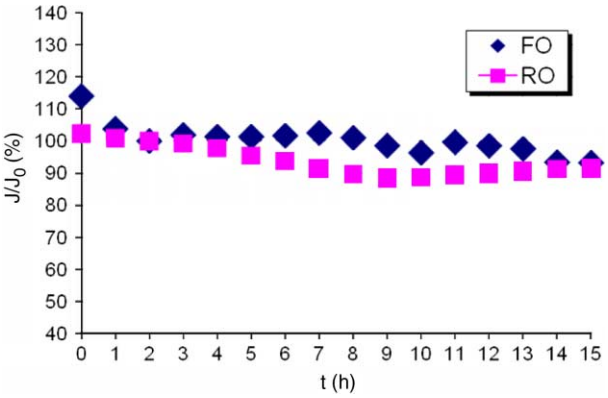

Figure 2 | Observed flux decline in FO and RO, J_0 (RO) = 12.8 LMH, J_0 (FO) = 11.6 LMH, Feed: 200 ppm SiO_2 in 1 g NaCl per L Milli-Q water.

below. The RO and FO experiments were conducted with the driving forces of 19.2 bar and 1.4 molal NaCl draw solution, respectively. From a previous study (She 2008), the water permeability constant of the membrane was found to be around $2.2 \cdot 10^{-7}$ ms^{-1} bar^{-1} at ambient temperature, which was relatively low compared to conventional RO composite membranes (Tang *et al.* 2007). This could explain the relatively low fluxes observed (about 13 Lm^{-2} h^{-1}) in this current study, which were in the same flux range for this type of membrane as reported in the literature (Holloway *et al.* 2007; Cornelissen *et al.* 2008; Achilli *et al.* 2009).

It was observed that the flux decline in RO was gradual and steady, which was consistent with the critical flux concept and also observed in the constant pressure RO studies (Tang *et al.* 2007). For FO, there was a sudden drop in flux initially, followed by a gentle decline. This behaviour was observed in repeated experiments, and the exact timing of this sudden drop in flux could vary within the first few hours of the experiments. We attribute this sudden flux drop behaviour in FO to the salt (NaCl) transport from the draw solution into the feed solution, which would elevate the feed-side osmotic pressure and aggravate fouling on the membrane surface (double layer compression at higher ionic strength), that in turn exacerbate the CEOP effect. Thereafter, however, the flux in FO was relatively stable. Visual examination of the membrane coupons after the experiments found white deposits on the membrane surface, which indicated that fouling had occurred in both RO and FO.

In general, slow flux decline was observed in both FO and RO under the given conditions. A common explanation for this could be the low experimental fluxes, which might have been around the critical flux for the particular feed conditions (Tang & Leckie 2007; Chong *et al.* 2008*b*). In addition, the membrane material was hydrophilic, and had a relatively low measured mean roughness around 35.7 nm (She 2008), which could alleviate fouling. These factors could also be contributing to the slow flux decline observed in the experiments.

Modelling results

To understand the slow flux decline phenomenon observed in FO, three scenarios were modelled (Figures 3–5). Both Figure 3 and Figure 4 represented possible operating conditions for water reclamation applications with the influent TDS of around 1 gL^{-1}. Whereas Figure 3 assumed that the salt transport in FO was negligible ($J_s = 0$)—an ideal assumption that was sometimes made in the literature (McCutcheon & Elimelech 2006) but unlikely to be valid especially for smaller size draw solutes such as NaCl, Figure 4 aimed to model a more realistic scenario. Here, J_s was assumed to be around 5 $gm^{-2}h^{-1}$, which would be a low to moderate value of the salt flux that was encountered in real applications (Achilli *et al.* 2009). Figure 5 simulated seawater desalination with the influent TDS in the range of 30 gL^{-1}. For consistency, $J_s = 5\,gm^{-2}h^{-1}$ was considered, though a higher J_s could be expected at higher draw solution concentration as predicted by the solutions diffusion theory. Other assumed parameters are found in Table 2.

The investigation was conducted assuming constant overall driving force operation, that is a constant feed pressure for RO, and a constant overall osmotic pressure difference (bulk feed to bulk draw solution) for FO. The performance is modelled as fouling progresses (the thickness of the fouling cake (δ_{cake}) increases). The results are organised into three presentations: (i) normalised flux in FO and RO, (ii) flux analysis in FO, and (iii) flux analysis in RO. Part (i) for each scenario was plotted by solving Equations (1) and (2) under the given conditions. Part (ii) and (iii) could be derived by re-arranging Equations (1) and (2) and apportioning the intrinsic flux given by the driving force into the components with the dimension [LMH]:

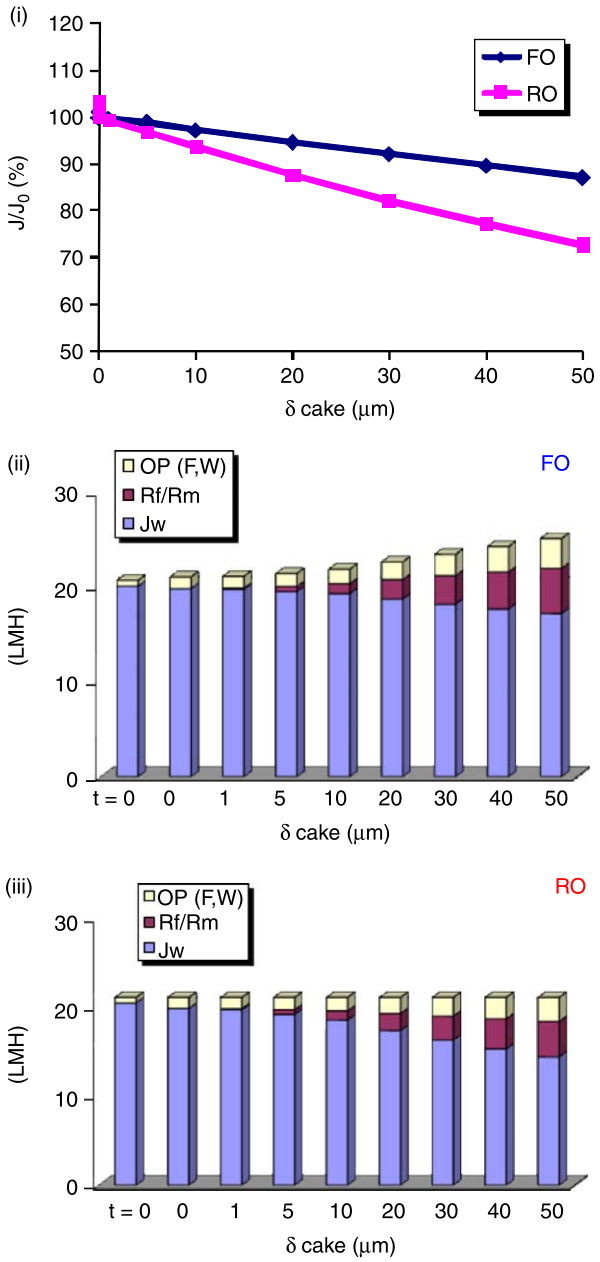

Figure 3 | Effects of fouling on modelled scenario for water reclamation ($J_s = 0\,gm^{-2}h^{-1}$): (i) flux decline FO vs RO, (ii) flux analysis for FO, (iii) flux analysis on RO; ($c_{F,0} = 1\,gL^{-1}$ NaCl, $c_{F,B} = 2\,gL^{-1}$ NaCl (RO = FO), $\Delta p = 26.6$ bar, $\pi_{D,B} = 104.5$ bar).

for permeating of the product flux (J_w), for overcoming of the normalised fouling resistance (R_f/R_m), and for accounting for the increased osmotic pressure on the feed-side of the membrane wall exacerbated by the CEOP effect ($OP_{(F,W)}$).

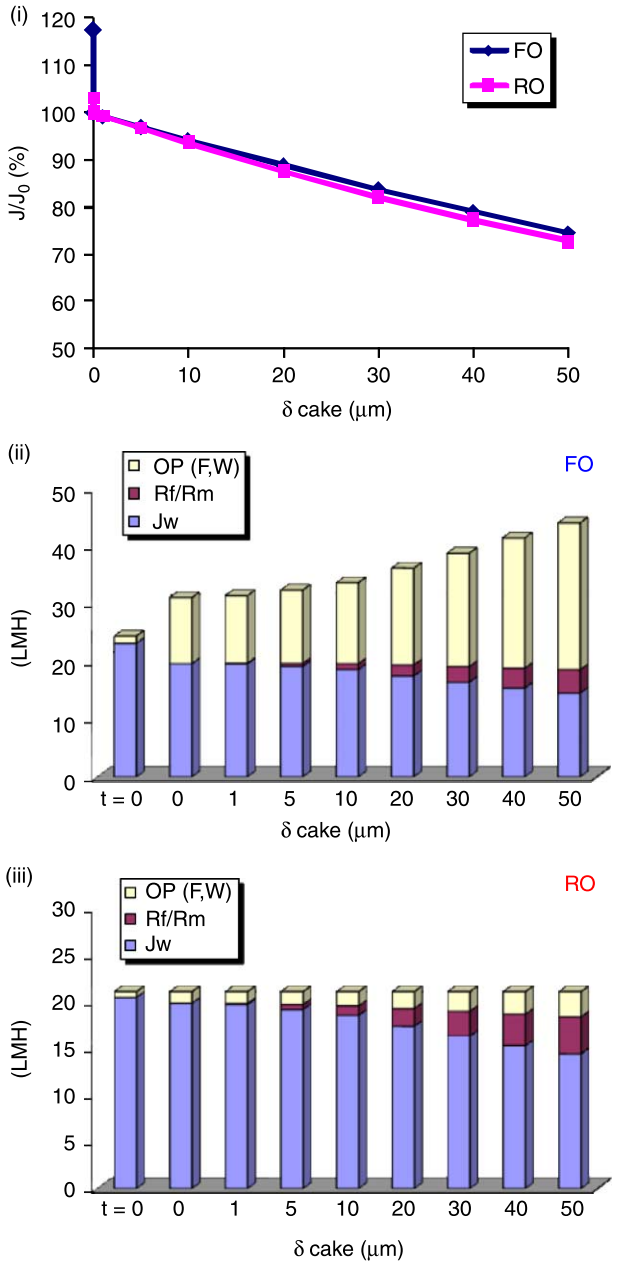

Figure 4 | Effects of fouling on modelled scenario for water reclamation ($J_s = 5\,gm^{-2}h^{-1}$): (i) flux decline FO vs RO, (ii) flux analysis for FO, (iii) flux analysis on RO; ($c_{F,0} = 1\,gL^{-1}$ NaCl, $c_{F,B} = 2\,gL^{-1}$ NaCl (RO), $c_{F,B} = 17.6\,gL^{-1}$ NaCl (FO), $\Delta p = 26.6$ bar, $\pi_{D,B} = 154.2$ bar).

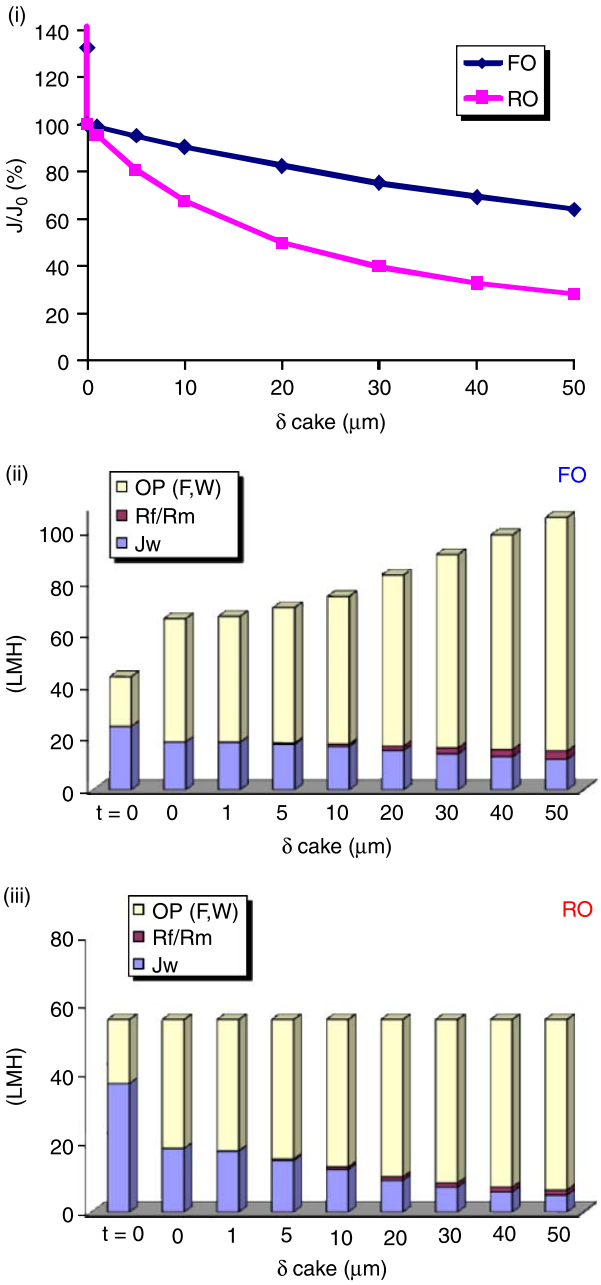

Figure 5 | Effects of fouling on modelled scenario for seawater desalination ($J_s = 5\,gm^{-2}h^{-1}$): (i) flux decline FO vs RO, (ii) flux analysis for FO, (iii) flux analysis on RO; ($c_{F,0} = 30\,gL^{-1}$ NaCl, $c_{F,B} = 60\,gL^{-1}$ NaCl (RO), $c_{F,B} = 75.6\,gL^{-1}$ NaCl (FO), $\Delta p = 70.4$ bar, $\pi_{D,B} = 300$ bar).

The model also considered the salt concentration effect as discussed above. Even when fouling had not yet occurred, the steady-state feed concentration ($c_{F,B}$ @ $\delta_{cake} = 0$) would be higher than its influent concentration ($c_{F,0}$ @ $t = 0$) as given by Equation (3) due to the concentration factor imposed by the recovery (ϕ). The steady-state value is dependent on a number of parameters, such that $c_{F,B}\uparrow$ as $\phi\uparrow$, $J_s\uparrow$, $J_w\downarrow$ and $c_{F,0}\uparrow$. Here, some elaboration for FO is necessary: firstly, although a higher $c_{F,0}$ results in a higher $c_{F,B}$ in absolute terms, the relative impact of J_s on $c_{F,B}$ is actually

Table 2 | Common parameters assumed in the modelling

Model foulant: 20 nm SiO_2 ($\rho_p = 2.6\,g\,cm^{-3}$, $\epsilon_c = 0.4$, $\tau_c = 2.5$, $\alpha_c = 1.6{\cdot}10^{15}\,mkg^{-1}$)
$A = 2.2{\cdot}10^{-7}\,ms^{-1}\,bar^{-1}$
$B = 1.8{\cdot}10^{-7}\,ms^{-1}$
$D = 1.61{\cdot}10^{-9}\,m^2\,s^{-1}$
$S = 0.4{\cdot}10^{-3}\,m$
$\phi = 0.5$
$J_w\ (t = 0) \sim 20$ LMH

mitigated by a higher $c_{F,0}$; and secondly, a higher J_w would reduce $c_{F,B}$, but it would also negatively affect driving force due to a greater ICP (Equation (2)), so a trade-off would be needed. Here, $J_w \sim 20$ LMH is assumed.

For scenario Figure 3, where $J_s = 0$, the salt concentration effect in FO equals that in RO (Equation (3)). From 3-(i), a slower flux decline could be observed in FO as compared to RO. It can be seen from 3-(ii) and 3-(iii) that as fouling progresses, the magnitudes of $OP_{(F,W)}$ and R_f/R_m increase comparably in both FO and RO. For illustration, at $t = 0$, the intrinsic flux given by the driving force for FO (3-(ii)) = 20.7 LMH, which comprises the actual permeating flux = 20.1 LMH (J_w) and the flux loss due to the feed-side osmotic pressure on the membrane wall = 0.6 LMH ($OP_{(F,W)}$). As the equilibrium of the feed concentration is attained but fouling has not yet set in ($\delta_{cake} = 0\,\mu m$), the feed-side osmotic pressure increases due to the salt concentration effect ($\phi = 0.5$). The intrinsic flux is then 21.0 LMH = 19.8 LMH (J_w) + 1.2 LMH ($OP_{(F,W)}$). As fouling progresses, for example at $\delta_{cake} = 5\,\mu m$, the intrinsic flux for FO is 21.4 LMH = 19.5 LMH (J_w) + 0.5 LMH (R_f/R_m) + 1.4 LMH ($OP_{(F,W)}$). Similarly for RO (3-(iii)): @ $t = 0$, the intrinsic flux given by the driving force is 21.0 LMH = 20.4 LMH (J_w) + 0.6 LMH ($OP_{(F,W)}$); @ $\delta_{cake} = 0\,\mu m$, the intrinsic flux for RO is 21.0 LMH = 19.8 LMH (J_w) + 1.2 LMH ($OP_{(F,W)}$); @ $\delta_{cake} = 5\,\mu m$, the intrinsic flux for RO is 21.0 LMH = 19.1 LMH (J_w) + 0.5 LMH (R_f/R_m) + 1.4 LMH ($OP_{(F,W)}$). What these examples illustrate is that at the same bulk feed concentration ($c_{F,B}$) and similar level of fouling (CEOP and R_f/R_m), FO is expected to give slower flux decline than RO. This is because while the effective driving force for RO is constant (Δp in Equation (1)), the effective driving force for FO actually increases with reducing flux, as the effect of ICP lessens (Equation (2): ICP $\sim \exp(-J_w)$). The result of this is that the flux decline in RO increases non-linearly under the double action of R_f and CEOP, whereas the flux decline in FO is mitigated by the ICP.

In Figure 4, where $J_s = 5\,gm^{-2}\,h^{-1}$ is assumed, the salt concentration effect in FO ($c_{F,B} = 17.6\,gL^{-1}$ @ $\phi = 0.5$) is significantly greater than that in RO ($c_{F,B} = 2\,gL^{-1}$ @ $\phi = 0.5$), as opposed to the observation in Figure 3. The increase in the bulk feed concentration ($c_{F,B}$) accounts for the initial flux drop observed in FO between $t = 0$ (influent) and $\delta_{cake} = 0$ (steady-state) due to the increased osmotic pressure of the feed solution. As fouling progresses, the effective driving force in FO increases due to the effect of the reduced ICP at lower membrane flux, but $OP_{(F,W)}$ also gets excessively exacerbated due to the more severe CEOP effect caused by the increased feed osmotic pressure. The overall result is that similar rate of flux decline may be expected in both FO and RO (4-(i) to -(iii)), which is also in agreement with our experimental observation (Figure 2). The importance of salt transmission can be seen by comparing 3-(i) to 4-(i). For $J_s = 0\,gm^{-2}\,h^{-1}$, the normalised flux at $\delta_{cake} = 50\,\mu m$ drops to 87%, and for $J_s = 5\,gm^{-2}\,h^{-1}$, the normalised flux at $\delta_{cake} = 50\,\mu m$ drops to 75%. The need for low transmission FO membranes is evident from this analysis.

For scenario Figure 5, at the same J_s as in Figure 4 but higher $c_{F,0}$, the relative impact of the salt concentration effect in FO ($c_{F,B} = 75.6\,gL^{-1}$ @ $\phi = 0.5$) lessens according to Equation (3), and is marginally greater than that in RO ($c_{F,B} = 60\,gL^{-1}$ @ $\phi = 0.5$). In a way, Figure 5 is analogous to Figure 3 in that the bulk feed concentration ($c_{F,B}$) of RO vs. FO is fairly similar. The difference is that the CEOP effect is now much more severe due to the higher feed osmotic pressure. This did not affect the analysis under the same level of fouling, and a slower flux decline could be observed in FO as compared to RO. The explanation for this is again due to the mitigating effect of the ICP for FO as flux reduces (5-(i) to -(iii)).

The above discussion can be illustrated using a pure water flux–driving force diagram as presented in Figure 6. Here, the graph for RO is linear, and the gradient of this line is the water permeability constant of the membrane

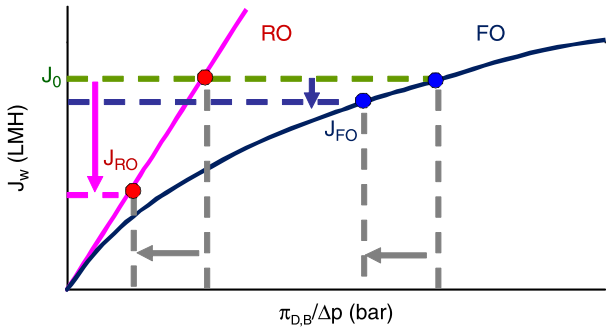

Figure 6 | Effect of equal loss of driving force on flux in FO and RO.

($J_w = A{\cdot}\Delta p$, Equation (1)). For FO, the graph is logarithmic with $J_w = (A{\cdot}\pi_{D,B} + B){\cdot}\exp(-J_w{\cdot}S/D)$ (Equation 2). Due to the curvature of the graphs, it can be observed that at the same initial flux (J_0) and under equal loss of driving force, the flux decline in FO is consistently smaller than that in RO, regardless of the nature of the fouling cake that is occurring. However, this benefit can be negated by the transmission of the draw solutes, which elevates feed-side osmotic pressure and then exacerbates the loss in driving force via the CEOP effect. It is evident that the transmission of draw solutes (salt transport) can have significant effect on FO performance, and has to be minimised.

CONCLUSIONS

This study investigated flux behaviour in FO and RO under similar fouling conditions based on a combined experimental-modelling approach. It was found that at relatively low fluxes between 12 and 14 LMH, both RO and FO exhibited slow flux decline. Therefore, the slower flux decline commonly observed in FO experiments did not prove lesser fouling cake compaction as compared to the pressure driven membrane processes. There could be other contributing factors to this such as the use of hydrophilic and smooth membranes, and the counteracting effect of ICP. Experimentally, an initial drop in flux was observed for FO, which could be attributed to the NaCl transport from the draw solution into the feed solution that could have increased the osmotic pressure on the membrane feed-wall, aggravated fouling and exacerbated the CEOP effect. The modelling analysis complemented experimental findings. For FO, the effect of fouling and flux decline is to reduce ICP due to reduced flux. This provides an increase in the effective driving force that partially compensates for the fouling resistance. This does not apply for RO. It was also established that the transmission of draw solutes from the draw solution into the feed can have significant effect on FO performance. Consequently, an important attribute of an appropriate draw solution for FO is to have minimal draw solute transmission through the membrane. However, if NaCl solution is used, then the membranes used in FO application need to be improved to substantially reduce this salt transport.

ACKNOWLEDGEMENTS

The authors acknowledge and thank: Hew Sock Fang and She Qian Hong for the performance of the experimental work as part of their studies at the NTU, Hydration Technologies Innovations (HTI) for the friendly communication and provision of FO membranes, the Environment and Water Industry Development Council (EWI) and the PUB of Singapore for support to the Singapore Membrane Technology Centre (SMTC) and for the PhD scholarship awarded to Winson C.L. Lay.

REFERENCES

Achilli, A., Cath, T. Y., Marchand, E. A. & Childress, A. E. 2009 The forward osmosis membrane bioreactor: a low fouling alternative to MBR processes. *Desalination* **239**(1–3), 10–21.

Cath, T. Y., Childress, A. E. & Elimelech, M. 2006 Forward osmosis: principles, applications, and recent developments. *J. Memb. Sci.* **281**(1–2), 70–87.

Chong, T. H., Wong, F. S. & Fane, A. G. 2008*a* The effect of imposed flux on biofouling in reverse osmosis: role of concentration polarisation and biofilm enhanced osmotic pressure phenomena. *J. Memb. Sci.* **325**(2), 840–850.

Chong, T. H., Wong, F. S. & Fane, A. G. 2008*b* Implications of critical flux and cake enhanced osmotic pressure (CEOP) on colloidal fouling in reverse osmosis: experimental observations. *J. Memb. Sci.* **314**(1–2), 101–111.

Cornelissen, E. R., Harmsen, D., de Korte, K. F., Ruiken, C. J., Qin, J. J., Oo, H. & Wessels, L. P. 2008 Membrane fouling and process performance of forward osmosis membranes on activated sludge. *J. Memb. Sci.* **319**(1–2), 158–168.

Field, R. W., Wu, D., Howell, J. A. & Gupta, B. B. 1995 Critical flux concept for microfiltration fouling. *J. Memb. Sci.* **100**(3), 259–272.

Gerstandt, K., Peinemann, K. V., Skilhagen, S. E., Thorsen, T. & Holt, T. 2008 Membrane processes in energy supply for an osmotic power plant. *Desalination* **224**(1–3), 64–70.

Hoek, E. M. V. & Elimelech, M. 2003 Cake-enhanced concentration polarization: a new fouling mechanism for salt-rejecting membranes. *Environ. Sci. Technol.* **37**(24), 5581–5588.

Holloway, R. W., Childress, A. E., Dennett, K. E. & Cath, T. Y. 2007 Forward osmosis for concentration of anaerobic digester centrate. *Water Res.* **41**(17), 4005–4014.

Lee, K. L., Baker, R. W. & Lonsdale, H. K. 1981 Membranes for power generation by pressure-retarded osmosis. *J. Memb. Sci.* **8**(2), 141–171.

Loeb, S., Titelman, L., Korngold, E. & Freiman, J. 1997 Effect of porous support fabric on osmosis through a Loeb-Sourirajan type asymmetric membrane. *J. Memb. Sci.* **129**(2), 243–249.

McCutcheon, J. R. & Elimelech, M. 2006 Influence of concentrative and dilutive internal concentration polarization on flux behavior in forward osmosis. *J. Memb. Sci.* **284**(1–2), 237–247.

McCutcheon, J. R. & Elimelech, M. 2007 Modeling water flux in forward osmosis: implications for improved membrane design. *AIChE J.* **53**(7), 1736–1744.

McCutcheon, J. R., McGinnis, R. L. & Elimelech, M. 2005 A novel ammonia-carbon dioxide forward (direct) osmosis desalination process. *Desalination* **174**(1), 1–11.

Oo, M. H., Kekre, K., Tao, G. H., Qin, J. J., Lay, C. L., Lew, C. H., Cornelissen, E. R., Ruiken, C. J., Korte, K. F. d. & Wessels, L. P. 2008 Osmotic Membrane Bioreactor: Preliminary Pilot Study on Effects of Osmotic Pressure on Membrane Flux and Air Scouring on Fouling. IWA Regional Conference Membrane Technologies in Water and Waste Water Treatment. Moscow.

Robinson, R. A. & Stokes, R. H. 2002 *Electrolyte Solutions, Second Revised Edition*. Dover Publications, Mineola, NY.

She, Q. H. 2008 Effect of Hydrodynamic Conditions and Feedwater Composition on Fouling of Ultrafiltration and Forward Osmosis Membranes by Organic Macromolecules, Nanyang Technological University. M.Eng. Thesis.

Tang, C. Y., Kwon, Y.-N. & Leckie, J. O. 2007 Fouling of reverse osmosis and nanofiltration membranes by humic acid–Effects of solution composition and hydrodynamic conditions. *J. Memb. Sci.* **290**(1–2), 86–94.

Tang, C. Y. & Leckie, J. O. 2007 Membrane independent limiting flux for RO and NF membranes fouled by humic acid. *Environ. Sci. Technol.* **41**(13), 4767–4773.

Wessels, L. P. & Cornelissen, E. R. 2005 Werkwije en inrichting voor het in een membraan-filtratie-eenheid behandelen van een waterige afvalstroom afkomstig van een bioreactor (Dutch Patent NL1028484). Netherlands.

Zhang, Y. P., Chong, T. H., Fane, A. G., Law, A., Coster, H. G. L. & Winters, H. 2008 Implications of enhancing critical flux of particulates by AC fields in RO desalination and reclamation. *Desalination* **220**(1–3), 371–379.